

# Topological phase transitions in bulk.

Stanislav Chadov<sup>\*1</sup>, Janos Kiss<sup>1</sup>, Jürgen Kübler<sup>2</sup>, Claudia Felser<sup>1</sup>

<sup>1</sup> Max-Planck-Institut für Chemische Physik fester Stoffe, Nöthnitzer Str. 40, 01187 Dresden, Germany

<sup>2</sup> Institut für Festkörperphysik, Technische Universität Darmstadt, 64289 Darmstadt, Germany

Received XXXX, revised XXXX, accepted XXXX

Published online XXXX

**Key words:** topological insulator, random disorder, electron localization, CPA

\* Corresponding author: e-mail stanislav.chadov@cpfs.mpg.de, Phone: +49-0351-46462238, Fax: +49-0351-46463002

We consider the analogy between the topological phase transition which occurs as a function of spatial coordinate on a surface of a non-trivial insulator, and the one which occurs in the bulk due to the change of internal parameters (such as crystal field and spin-orbit coupling). In both cases the system exhibits a Dirac cone, which is the universal manifestation of topological phase transition, independently on the type of driving parameters. In particular, this leads to a simple way of determining the topological class based solely on the bulk information even for the systems with translational symmetry broken by atomic disorder or by strong electron correlations. Here we demonstrate this on example of the zinc-blende related semiconductors by means of the *ab-initio* fully-relativistic band structure calculations involving the coherent potential approximation (CPA) technique.

Copyright line will be provided by the publisher

**1 Introduction.** The remarkable ability of the semiconductors with topologically non-trivial band structure (for the overview see e.g. Ref. [1]) to exhibit the non-dissipative quantized surface spin-current attracts great attention both in theoretical physics, material science and spintronics engineering. This spin-current is represented by a pair of opposite charge currents carrying opposite spin states. Each charge current is induced by the intrinsic spin-orbit interaction, which can be viewed as spin-dependent effective magnetic field. These effective magnetic fields quantize the electron orbits into the Landau levels, which leads to a quantization of the resulting spin-current in units of  $(1/2 + n) (e^2/h)$ . The absence of dissipation holds as long as the structure of the Landau levels is preserved which is guaranteed by the time-reversal symmetry. In contrast to the bulk, the non-compensated spin-current can be observed and detected on the surface, due to the space-reversal symmetry break while keeping the time-reversal symmetry. On the surface the system exhibits the Dirac cone, which can be observed directly by the angular-resolved photoemission technique. This property of topological insulators is typically exploited in the band structure calculations in order to probe the non-trivial nature of the material. On the other hand, the reliable surface calculations most often appear to be extremely resource demanding. Alternatively, since the topological edge states

emerge from the non-trivial bulk band structure, it must be a way for determining the topological class based on pure bulk information. Indeed, it is possible to calculate the topological invariant  $Z_2$  based on the parity analysis of the occupied eigenstates [2,3]. Obviously, this procedure cannot be applied in situations when the eigenstates do not exist due to the absence of the translational symmetry. The reasons for such symmetry break are typically the non-periodic boundary conditions, atomic (chemical or structural) disorder, or the intrinsic electronic disorder caused by strong dynamical correlations. The hint is that in the first case, i. e. on the surface of topological insulator one always observes the Dirac cone. At this moment it is important to understand that the surface is not just a complicated geometrical object with reduced dimensionality, potential step etc., but it is a transition between different bulk phases. The parameter of this transition is simply the spatial coordinate. In this context the Dirac cone is not an ingenuous surface phenomenon, but is rather a fundamental manifestation of the transition between two distinct topological phases in certain parameters space. Indeed, the Dirac cone can occur in the bulk band structure as well: all materials which appear at the borderline between topologically non-trivial and trivial phases exhibit the bulk Dirac cone [4]. This fact indicates that for materials with the translational symmetry broken by disorder the topolog-

Copyright line will be provided by the publisher

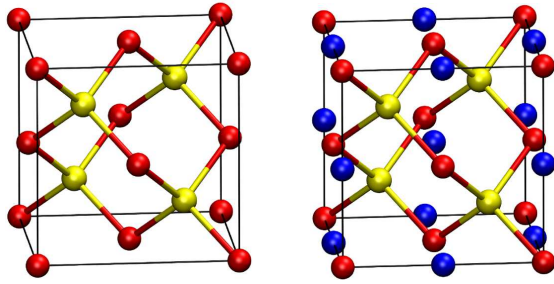


**Figure 1** (color online) Left: crystal structure of the zinc-blende binary YZ compound (space group No. 216). Yellow and red spheres represent the transition-metal Y and main-group elements Z. Right: by adding one more transition element X (blue sphere) one obtains ternary XYZ Heusler compound.

ically non-trivial state still can be determined based on the bulk information.

In the present work we would like to illustrate this fact by first-principles calculations taking into account the random disorder by means of the Coherent Potential Approximation (CPA) alloy theory [5,6]. Simultaneously, the CPA serves as adiabatic transition technique, which allows us to model the smooth transformation of one material into another and observe the details of the topological phase transition in the bulk. This transformation has also a physical relevance, i.e. it directly describes the effect of the random chemical substitution. As a real-case example we will consider the class of zinc-blende related structures, which contain a great manifold of non-trivial and trivial semiconductors in which the details of their band structures are well-known.

**2 Topologically non-trivial systems with zinc-blende structure.** Topological semimetals (or gapless semiconductors with topologically non-trivial band structure) represent a rich and at the same time rather simple class of materials, which allows to demonstrate the general trends specific for the class of the 2D topological insulators as a whole. The simplest systems in this class are the binaries with zinc-blende structure (see Fig. 1) as e.g. HgTe [7,8]. It is relatively easy to search for the nonmagnetic semiconductors in this class by picking the pairs of elements with average number of valence electrons per atom  $n_{\text{val}} = 6$  [4,9]. Without restriction one can add here the whole class of ternary Heusler semiconducting materials (so-called half-Heusler semiconductors) which possess the same space group No. 216 and are different from binaries by having one more transition metal element [4,9,10]. As it follows from these studies, all topologically-related physics of zinc-blende like compounds is contained in the vicinity of the  $\Gamma$ -point: all trivial semiconductors of this type exhibit a direct non-zero band gap, whereas all non-trivial materials are gapless. It is surprising, but there was

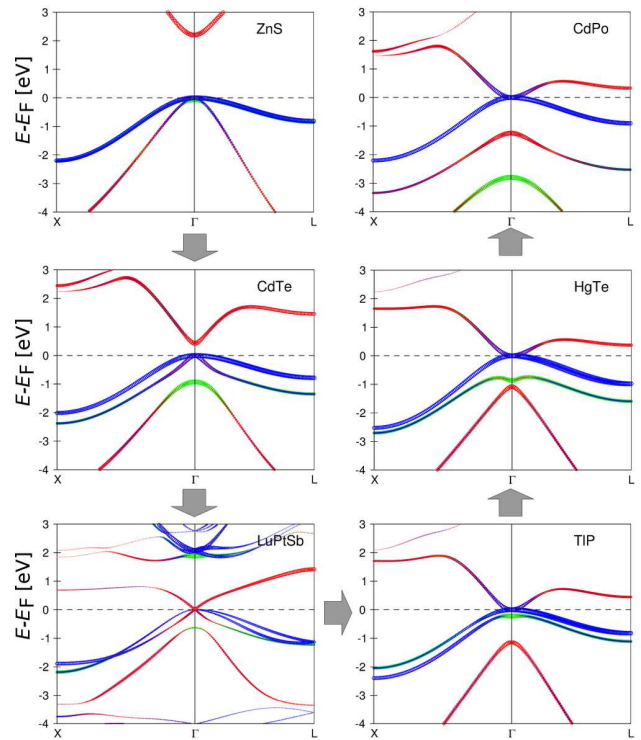


**Figure 2** (color online) Relativistic band structures calculated for the ordered YZ binary zinc-blende (ZnS, CdTe, TIP, HgTe and CdPo) and related ternary XYZ Heusler (LuPtSb) materials. Red, green and blue colors refer to the orbital symmetries  $s_{1/2}$  (carried by the transition element Y),  $p_{1/2}$  and  $p_{3/2}$  (carried by the main group element Z), respectively. The gray arrows indicate the transition from trivial semiconductors ZnS, CdTe towards topological phase transition marked by the Dirac cone (LuPtSb), and further into the class of the non-trivial gapless semiconductors TIP, HgTe and CdPo. Calculations are performed by the PY-LMTO method [11]. As the LDA [12] form of the exchange-correlation potential was used, the band gaps of trivial semiconductors (ZnS, CdTe) are underestimated.

no exception found yet. Here we also illustrate the difference between topological and trivial materials within this class in terms of the band structure, by giving few examples shown in Fig. 2. The trivial band structure is characterized by the empty  $s_{1/2}$  orbital of the transition metal atom Y and the fully filled  $p$ -shell of the main-group element Z, split into  $p_{3/2}$  and  $p_{1/2}$  by spin-orbit coupling. These compounds exhibit a non-zero direct band-gap at the Fermi energy and are represented by the light-element semiconductors with average nuclear number  $\langle Z \rangle$  roughly less than 60: e.g. ZnS ( $\langle Z \rangle = 23$ ), ZnSe ( $\langle Z \rangle = 32$ ), CdTe, ScPtSb ( $\langle Z \rangle = 50$ ); with certain exceptions, as e.g. LuNiBi ( $\langle Z \rangle \approx 60.7$ ) [4]. In the non-trivial systems the  $p_{3/2}$  orbital is half-filled, for this reason it sticks to the Fermi energy and within cubic

symmetry the system becomes zero-gap semiconductor. At the same time the  $p_{1/2}$  and  $s_{1/2}$  orbitals are fully occupied. This so-called band inversion changes the parity of the wave function which is directly related to the topological  $Z_2$  invariant. Such materials are typically heavy with  $\langle Z \rangle \gtrsim 60$ : ZnPo ( $\langle Z \rangle = 57$ ), HgTe and CdPo ( $\langle Z \rangle = 66$ ), YPtBi ( $\langle Z \rangle \approx 66.7$ ), LuPtBi ( $\langle Z \rangle \approx 77.3$ ) [4, 9]; with certain exceptions, as e. g. was found in present calculations for TIP ( $\langle Z \rangle = 48$ ). Interesting case is represented by the borderline compounds, such as YPdBi, YPtSb ( $\langle Z \rangle = 56$ ), or LuPtSb ( $\langle Z \rangle \approx 66.7$ ) [10], which exhibit the Dirac cone in the bulk, i. e. can be easily switched between topological or trivial states by small variations of the stoichiometry or the lattice constant [4].

Obviously, there is also a continuum of alloys, which can be obtained by combining various ordered zincblende ( $Y_{1-y}Y'_y$ )( $Z_{1-z}Z'_z$ ) or half-Heusler materials ( $X_{1-x}X'_x$ )( $Y_{1-y}Y'_y$ )( $Z_{1-z}Z'_z$ ). By varying the ratios of elements allows to tune the properties of the system continuously in a wide range. For example, by substituting Hg with Cd in ( $Hg_{1-x}Cd_x$ )Te series one obtains the zero-gap materials for  $x \lesssim 0.17$  and non-zero band gap for  $x \gtrsim 0.83$  [13], which correspond to the non-trivial and trivial regimes, respectively.

**3 Chemical disorder in terms of the CPA alloy theory.** In the context of the first-principles description of the electronic structure, the most practical way to treat the random disorder is by using the so-called Coherent Potential Approximation (CPA) [5, 6]. In fact, until now the CPA (and its extensions) remains the only technique which incorporates the effects of the energy-dependent shift and lifetime broadening – the essential features of the electron localization caused by chemical disorder, which are not accessible within other theories, as e. g. the VCA [14] or supercell calculations.

The idea of CPA can be sketched by considering the example of binary alloy  $A_xB_{1-x}$  ( $0 \leq x \leq 1$ ), with each lattice site occupied either by atomic sorts A or B with probabilities  $x$  or  $1 - x$ , respectively. For simplicity we let the atomic potential to be characterized by a single energy level,  $\epsilon_A$  and  $\epsilon_B$ , for each sort respectively. In the second quantization form the Hamiltonian of  $A_xB_{1-x}$  alloy  $H_{AB}$  can be written as

$$H_{AB} = \sum_k \epsilon_k a_k^\dagger a_k + \sum_i \epsilon_i a_i^\dagger a_i. \quad (1)$$

The first term represents the sum over the valence states indexed by their wave vectors  $k$  with kinetic energies  $\epsilon_k$ . The second term is the sum over the lattice sites  $i$ ;  $\epsilon_i$  is the randomly fluctuating variable, equal to  $\epsilon_A$  or  $\epsilon_B$  with probabilities  $x$  or  $1 - x$ , respectively.

The straightforward solution for such Hamiltonian represents a complicated many-body problem. To make it practically accessible, one needs to find an adequate mean-field approximation, i. e. to substitute the real disordered

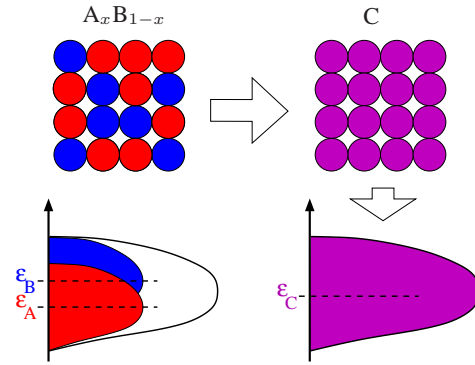


**Figure 3** (color online) Mean-field treatment of random disorder. Random binary  $A_xB_{1-x}$  alloy (A and B atoms are shown as red and blue spheres) is substituted by the regular array of the single effective atomic sort C (purple spheres). The effective potential  $\epsilon_C$  is adjusted in order to exhibit the same properties as the original disordered binary: for example, the same density of states.

system  $A_xB_{1-x}$  by the effective regular system C

$$\begin{aligned} H_{AB} &\approx H_C = \sum_k \epsilon_k a_k^\dagger a_k + \sum_i \epsilon_C a_i^\dagger a_i \\ &= \sum_k \epsilon_k a_k^\dagger a_k + \epsilon_C \sum_i a_i^\dagger a_i, \end{aligned} \quad (2)$$

which emulates the same properties. This idea is sketched on Fig. 3. The quality of such emulation is a matter of how the effective potential  $\epsilon_C$  is adjusted. It is easy to show, for example, that the straightforward averaging over the single-site potentials misses much of important physics. Indeed, since both  $\epsilon_A$  and  $\epsilon_B$  are the real-valued quantities, the effective regular potential  $\epsilon_C = x \cdot \epsilon_A + (1 - x) \cdot \epsilon_B$  will be real-valued as well. Thus, the solutions of the corresponding Schrödinger equation will be the delocalized Bloch waves which propagate without scattering and always lead to an infinite residual conductivity in case of a metal.

The CPA is based on a more rational choice of the mean-field variable by using the one-particle Green's function  $G_{AB}$ . Since it represents a response of the whole system to the  $\delta$ -like perturbation, i. e.

$$[\epsilon - H_{AB}(\mathbf{r})] G_{AB}(\mathbf{r}, \mathbf{r}', \epsilon) = \delta(\mathbf{r} - \mathbf{r}'), \quad (3)$$

it can be seen as a weighted superposition of responses from all configurations  $\Omega$  present in the system:

$$G_{AB} = \sum_\Omega x_\Omega G_\Omega, \quad \sum_\Omega x_\Omega = 1. \quad (4)$$

Each configuration  $\Omega$  can be presented as a perturbation of the effective regular system C, i. e. it can be defined using the Dyson equation:

$$\begin{aligned} G_\Omega &= G_C + G_C \sum_i (\epsilon_{i,\Omega} - \epsilon_C) G_\Omega \\ &= G_C + G_C T_\Omega G_C, \end{aligned} \quad (5)$$

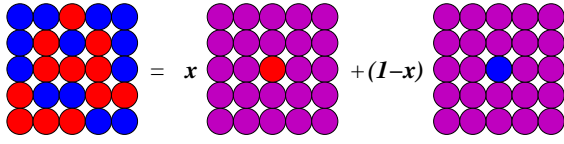


**Figure 4** (color online) Single-site CPA. Random binary  $A_{1-x}B_x$  alloy (A and B atoms are shown as red and blue spheres) is approximated as a superposition of two random impurity Green's functions (the impurities of types A and B are embedded in the regular host of the effective atoms C shown in purple) weighted with corresponding concentrations  $x$  and  $1 - x$ .

where  $\epsilon_{i,\Omega}$  is equal  $\epsilon_A$  or  $\epsilon_B$ , depending on the configuration  $\Omega$ ; the perturbation with respect to the regular system C is fully described by the term

$$\begin{aligned}
 T_\Omega &= \sum_i (\epsilon_{i,\Omega} - \epsilon_C) + \\
 &+ \sum_{i,j} (\epsilon_{i,\Omega} - \epsilon_C) G_C(\epsilon_{j,\Omega} - \epsilon_C) + \dots \\
 &= \frac{\sum_i (\epsilon_{i,\Omega} - \epsilon_C)}{1 - \sum_i (\epsilon_{i,\Omega} - \epsilon_C) G_C}. \quad (6)
 \end{aligned}$$

Thus, the requirement

$$G_{AB} = G_C \quad (7)$$

is equivalent to the cancellation of all partial perturbations in a total sum

$$\sum_\Omega x_\Omega T_\Omega = 0, \quad (8)$$

which completes the self-consistent set of equations, needed to determine  $\epsilon_C$ . Since the definition (6) involves the Green's function  $G_C$ , which is complex-valued and energy-dependent, the effective potential  $\epsilon_C$  appears to be complex-valued and energy-dependent as well. Its real part  $\text{Re } \epsilon_C$  defines the energy position of the electronic state, whereas the imaginary part  $\text{Im } \epsilon_C$  is responsible for its finite lifetime broadening caused by disorder. The latter is the necessary ingredient for the calculation of residual conductivity (except of the Berry phase contribution [15] which is a pure band structure effect). At the same time, the effective system formally remains to be translational invariant, thus once  $\epsilon_C$  is determined, we can restrict all further calculations to the primitive unit cell.

In order to simplify the set of the mean-field equations (5, 6, 8) we assume further that the only important configurations are those where the atoms are placed fully randomly, i. e. without certain nearest environment preference. In this case, only two configurations are left: random single impurities of type A and of type B, embedded in the C host (see Figure 4). Thus, the shortcoming of the single-site CPA is the absence of local environment effects. The latter can be, however, taken into account by its non-local extensions [16, 17, 18]. On the other hand, for the case of

random isovalent substitution, the single-site CPA remains a quite reasonable approximation even in the diluted limit, since the isovalent atoms intermix without extra environmental preference. The only condition is to preserve the zinc-blende structure which is again guaranteed by isovalency.

In the following all electronic structure calculations were carried out using the fully-relativistic Korringa-Kohn-Rostoker (KKR) Green's function method implemented within the SPR-KKR package [19] employing the density functional theory framework. Due to the multiple-scattering construction of the Green's function [20], the method provides a suitable base for mean-field approaches like CPA. Since the electronic structure of disordered materials in general does not show well defined Bloch eigenstates, their electronic structure is described by the Bloch-spectral function (BSF) defined by the imaginary part of the alloy Green's function that is diagonal in momentum space [20]. The exchange and correlation was treated using the Vosko-Wilk-Nusair form of the local density approximation (LDA) [12]. LDA is known for its typical underestimation of the band gaps of semiconductors. However, in case of our study this issue is not critical, since the observed trends are qualitatively well described even with LDA.

#### 4 Topological bulk phase transition induced by chemical substitution.

In the following we will track the evolution of the BSF driven by random chemical substitution along three distinct adiabatic paths, as depicted in Fig. 5, first by going between the pair of trivial, second - between the pair of non-trivial materials. In the third case we span the path from the non-trivial to the trivial one in order to study the details of the topological phase transition. In order to keep the conditions of adiabatic transition we perform the random substitution in isovalent manner, by keeping the chemical bonding rules and the crystal structure: i. e.  $YZ \rightarrow (Y_{1-x}Y'_x)(Z_{1-x}Z'_x) \rightarrow Y'Z'$ . For the alloy series the lattice constant is approximated linearly between the experimental constants for the pure materials.

As an example for the first case, we select two trivial materials, namely CdTe and ZnSe which are well-known semiconductors with non-zero band gaps. Both systems exhibit the same band structure features (Fig. 6): the conduction band is formed by the  $s_{1/2}$ -symmetry ( $5s$  for Cd and  $4s$  for Zn), whereas the top of the valence band carries the  $p_{3/2}$  symmetry ( $5p$  and  $4p$  orbitals for Te and Se, respectively). As it follows from the BSFs for the intermediate compositions, the random substitution of Cd by isovalent Zn and Te by isovalent Se does not change the energy distribution of the orbital characters, thus all the alloys in between exhibit similar band structures. On the other hand, one can easily notice their principle difference from the ordered materials: for  $0 < x < 1$  the symmetry analysis of eigenvalues cannot be applied directly, since there are no pure Bloch eigenstates, i. e. in the disordered regime the  $\delta$ -like poles

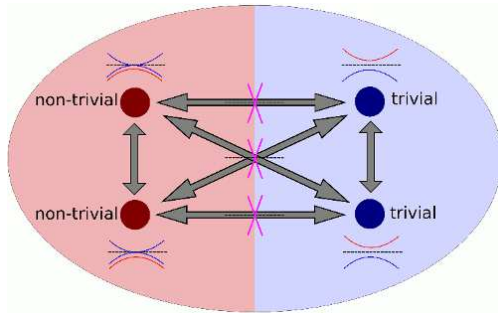


**Figure 5** (color online) Schematic illustration of the topological phase transition via substitution. Light red and blue areas distinguish between manifolds of topologically non-trivial and trivial materials, respectively. The corresponding band structures are schematically given in the vicinity of the red and blue spheres which indicate certain compounds from topological and trivial manifolds, respectively. The arrows indicate the transformation of one material into the other, e. g. by chemical substitution or by overgoing through the interface. The Dirac cone indicated by light purple lines always appears for the borderline case.

of the BSF turn into overlapping Lorentzians, spread over the whole  $k$ -space. Despite that we still can trace the evolution of their maxima in analogy to dispersion relation for the pure material, the only strict fact which tells us that all these materials belong to the same topological class is the absence of the Dirac-like dispersion within these series.

In the second case we transform the topologically non-trivial HgTe into another non-trivial zinc-blende system CdPo. The Po zinc-blende compounds (CdPo, ZnPo) were not considered earlier in the context of topology, however their crystal and band structures are well-known long ago [21,22]. As the presently calculated band structures show, CdPo is a gapless semiconductor with the bands alignment equivalent to HgTe (see Fig. 2). As it follows from the calculated series shown on Fig. 7, the situation is in principle very similar to the first case, with only difference that all materials belong to the non-trivial topological class, i. e.  $(\text{Hg}_x\text{Cd}_{1-x})(\text{Te}_x\text{Po}_{1-x})$ ,  $(0 < x < 1)$  remain gapless semiconductors and none of them exhibits the Dirac cone. On the other hand, it is interesting to admit, that due to different energy placements of the  $s$ -state in pure HgTe and CdPo compounds one observes the cone-like feature for the composition  $x \approx 0.3$  at about -1.5 eV. Indeed, in case of HgTe the  $s$ -state is situated below both  $p_{1/2}$  and  $p_{3/2}$  and in case of CdPo - right in between (see Fig. 2). By substituting Te to Po, the effective spin-orbit split increases by pushing the  $p_{1/2}$ -character down in energy until it interchanges its position with  $s$ -character state at  $x \approx 0.3$ . Since this re-ordering of the states is not connected with their re-occupation, the parity of the total wave function does not change and the rest of the alloy series remains in the same topological class.

In the last case the adiabatic path is going from the non-trivial CdPo to the trivial ZnSe semiconductor. As it follows from BSFs calculated for the series  $(\text{Cd}_{1-x}\text{Zn}_x)(\text{Po}_{1-x}\text{Se}_x)$  (Fig. 8), we indeed encounter certain composition ( $x_c \approx 0.72$ ) characterized by the bulk Dirac cone. All other alloys with  $x < 0.72$  are gapless semiconductors and topologically non-trivial, whereas those for  $x > 0.72$  are in the trivial regime, with the non-zero band gap. We briefly describe the most important steps of the BSF evolution in the vicinity of the  $\Gamma$  point: the Po  $6p$ -band is split due to spin-orbit coupling into a  $p_{3/2}$ -state (of  $\Gamma_8$  symmetry in the pure case) sitting right at the Fermi energy and a  $p_{1/2}$ -state (of  $\Gamma_7$  symmetry) which is about 3 eV lower. The Cd  $5s_{1/2}$  band (of  $\Gamma_6$  symmetry) is placed by the crystal field in between, at about -2 eV. Since by substitution we effectively decrease the spin-orbit coupling and increase the crystal field, both  $p_{1/2}$  and  $s_{1/2}$ -like states rise in energy by shifting towards the Fermi level. At the “critical” composition  $x_c = 0.72$  the system undergoes a topological phase transition manifested by the Dirac cone formed by a mixture of  $p$ - and  $s$ -symmetric states.

Due to the extremely deep energy position of the Cd  $s$ -shell in CdPo compound (approximately at -2 eV), the topological phase transition occurs within rather ZnSe-rich regime  $x_c = 0.72 > 0.5$ , which is not so severely disordered as in case of  $x = 0.5$ . Indeed, as it follows from the similar adiabatic path connecting non-trivial HgTe with trivial ZnSe semiconductor (see Fig. 9), the borderline concentration is shifted towards non-trivial regime since the  $s$ -symmetric state of the pure non-trivial alloy component is situated closer to the Fermi energy. Despite that the borderline composition is then shifted closer to the maximally disordered system  $x_c = 0.63 \approx 0.5$ , the Dirac cone exhibits rather well-defined Bloch-like states compared to the rest of the band structure.

Obviously, that the edge states with linear dispersion at the surface of a topological insulator and the states forming the Dirac cone in the bulk manifest the same transition phenomenon. The qualitative difference is only that due to the remaining effective translational symmetry (the difference is that the electrons are localized by disorder and are not Bloch-like), we observe two replica of Dirac cones with opposite spins on top of one another, whereas due to the break of space-reversal symmetry at the surface only a single cone remains, which exposes the adiabatic spin-current.

**Acknowledgements** Financial support by the DFG project FOR 1464 ASPIMATT (1.2-A) is gratefully acknowledged.

## References

- [1] M. Z. Hasan and C. L. Kane, Rev. Mod. Phys. **82**, 3045–3067 (2010).
- [2] L. Fu, C. L. Kane, and E. J. Mele, Phys. Rev. Lett. **98**, 106803 (2007).
- [3] L. Fu and C. L. Kane, Phys. Rev. B **76**, 45302 (2007).

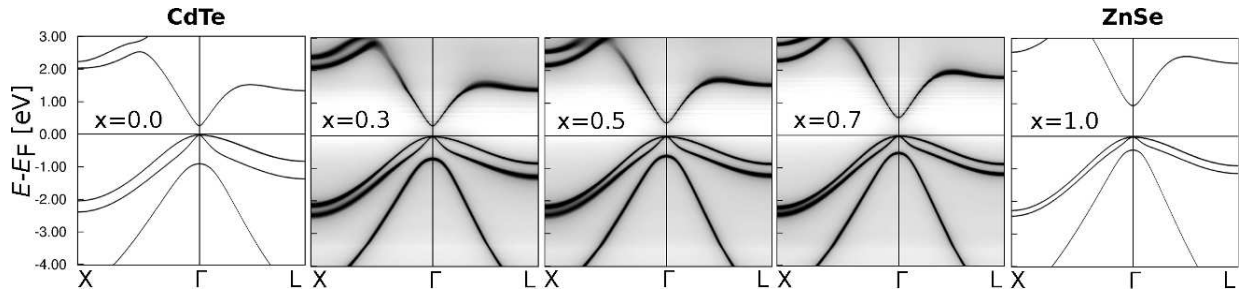


**Figure 6** Bloch-spectral functions calculated for the series of alloys  $(\text{Cd}_{1-x}\text{Zn}_x)(\text{Te}_{1-x}\text{Se}_x)$ ,  $x = 0, 0.3, 0.5, 0.7, 1$ . Since the pure compounds CdTe ( $x = 0$ ) and ZnSe ( $x = 1$ ) belong to the same topological (trivial) class, all intermediate compositions exhibit similar Bloch-spectral functions.

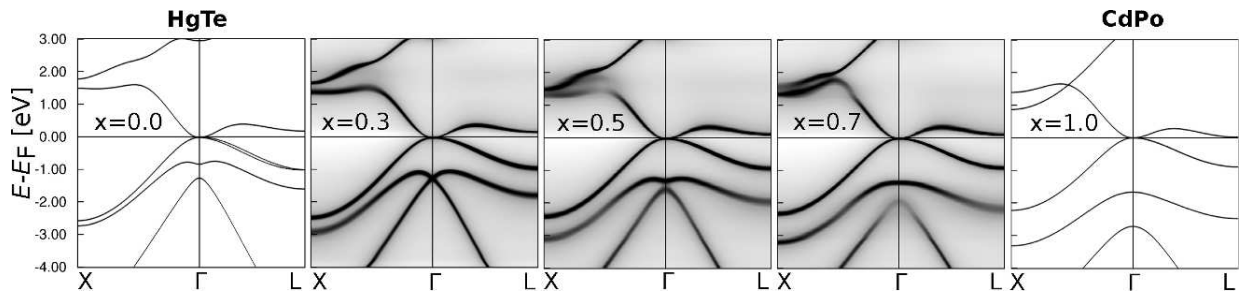


**Figure 7** Bloch-spectral functions calculated for the series of alloys  $(\text{Hg}_{1-x}\text{Cd}_x)(\text{Te}_{1-x}\text{Po}_x)$ ,  $x = 0, 0.3, 0.5, 0.7, 1$ . Since the pure compounds HgTe ( $x = 0$ ) and CdPo ( $x = 1$ ) belong to the same topological (non-trivial) class, all intermediate compositions exhibit similar gapless Bloch-spectral functions.

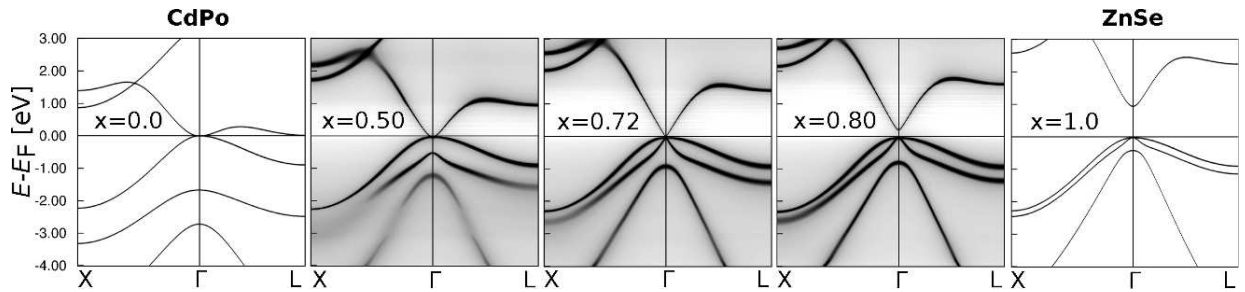


**Figure 8** Bloch-spectral functions calculated for the series of alloys  $(\text{Cd}_{1-x}\text{Zn}_x)(\text{Po}_{1-x}\text{Se}_x)$ ,  $x = 0, 0.5, 0.72, 0.8, 1$ . Since the pure compounds CdPo ( $x = 0$ ) and ZnSe ( $x = 1$ ) belong to different topological classes, there exists a certain intermediate composition which exhibits the topological phase transition state ( $x \approx 0.72$ ). All compositions  $x < 0.72$  are topologically non-trivial and characterized by zero-gap, whereas  $x > 0.72$  are trivial and exhibit a real band gap, which increases towards  $x = 1$ . The composition at  $x = 0.72$  is characterized by the clear Dirac cone centered at the Fermi energy.

- [4] S. Chadov, X. L. Qi, J. Kübler, G. H. Fecher, C. Felser, and S. C. Zhang, *Nature Materials* **9**, 541–545 (2010).  
 [5] P. Soven, *Phys. Rev.* **156**, 809–813 (1967).  
 [6] W. H. Butler, *Phys. Rev. B* **31**, 3260–3277 (1985).  
 [7] B. A. Bernevig, T. L. Hughes, and S. C. Zhang, *Science* **314**, 1757 (2006).  
 [8] M. König, S. Wiedmann, C. Brüne, A. Roth, H. Buhmann, L. Molenkamp, X. L. Qi, and S. C. Zhang, *Science* **318**, 766 (2007).

- [9] H. Lin, L. A. Wray, Y. Xia, S. Xu, S. Jia, R. J. Cava, A. Bansil, and M. Z. Hasan, *Nature Materials* **9**, 546–549 (2010).  
 [10] W. Al-Sawai, H. Lin, R. S. Markiewicz, L. A. Wray, Y. Xia, S. Y. Xu, M. Z. Hasan, and A. Bansil, *Phys. Rev. B* **82**, 125208 (2010).  
 [11] A. Perlov, A. Yaresko, and V. Antonov, Spin-polarized Relativistic Linear Muffin-tin Orbitals Package for Electronic Structure Calculations, PY-LMTO., unpublished).

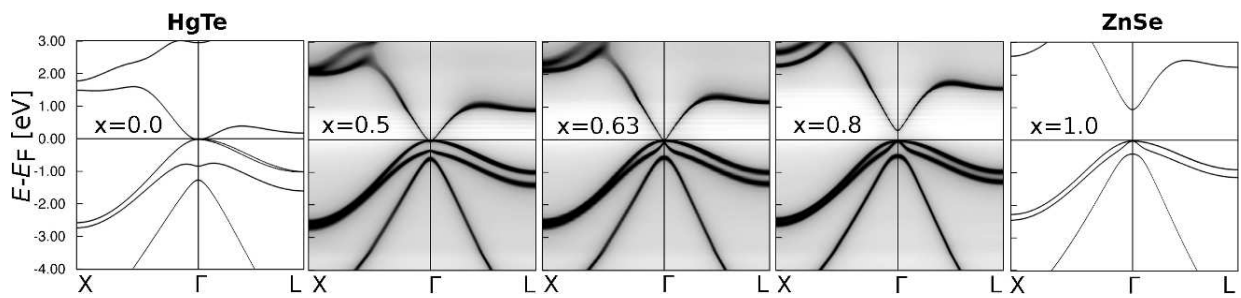


**Figure 9** Bloch-spectral functions calculated for the series of alloys  $(\text{Hg}_{1-x}\text{Zn}_x)(\text{Te}_{1-x}\text{Se}_x)$ ,  $x = 0, 0.5, 0.72, 0.8, 1$ . Since the pure compounds HgTe ( $x = 0$ ) and ZnSe ( $x = 1$ ) belong to different topological classes, there exists a certain intermediate composition which exhibits the topological phase transition state ( $x \approx 0.63$ ). All compositions  $x < 0.63$  are topologically non-trivial and characterized by zero-gap, whereas  $x > 0.63$  are trivial and exhibit a real band gap, which increases towards  $x = 1$ . The composition at  $x = 0.63$  is characterized by the clear Dirac cone centered at the Fermi energy.

- [12] S. H. Vosko, L. Wilk, and M. Nusair, *Can. J. Phys.* **58**, 1200 (1980).
- [13] J. Chu, S. Xu, and D. Tang, *Appl. Physics Lett.* **43**, 1064 (1983).
- [14] L. Nördheim, *Ann. Phys. (Leipzig)* **9**, 607 (1931).
- [15] D. Xiao, M. C. Chang, and Q. Niu, *Rev. Mod. Phys.* **82**, 1959–2007 (2010).
- [16] A. Mookerjee, V. K. Srivastavat, and V. Choudhry, *J. Phys. C: Solid State Phys.* **16**, 4555–4564 (1983).
- [17] C. I. Ventura and R. A. Barrio, *Physica B* **281-282**, 855–856 (2000).
- [18] D. A. Rowlands, J. B. Staunton, and B. L. Györfy, *Phys. Rev. B* **67**, 115109 (2003).
- [19] H. Ebert, D. Ködderitzsch, and J. Minár, *Rep. Prog. Phys.* **74(9)**, 096501 (2011).
- [20] J. S. Faulkner and G. M. Stocks, *Phys. Rev. B* **21**, 3222 (1980).
- [21] O. Madelung (ed.), *Semiconductors, Physics of IIVI and IVII Compounds, Semi-magnetic Semiconductors*, Landolt-Börnstein, New Series, Vol. III/17a, (Springer, Berlin, 1982).
- [22] A. Boukra, A. Zaoui, and M. Ferhat, *Solid State Commun.* **141**, 523–528 (2007).